Long-term evolution of the cold point tropical tropopause: Simulation results and attribution analysis

John Austin[1] and Thomas J. Reichler[2]

[1] The height, pressure, and temperature of the cold point tropical tropopause are examined in three 140 year simulations of a coupled chemistry climate model. Tropopause height increases approximately steadily in the simulations at a mean rate of 63 ± 3 m/decade (2σ confidence interval). The pressure trend changes near the year 2000 from -1.03 ± 0.30 hPa/decade in the past to -0.55 ± 0.06 hPa/decade for the future. The trend in tropopause temperature changes even more markedly from -0.13 ± 0.07 K/decade in the past to $+0.254 \pm 0.014$ K/decade in the future. The tropopause data were fit using regression by terms representing total column ozone, tropical mean sea surface temperatures, and tropical mass upwelling. Tropopause height and pressure closely follow the upwelling term, whereas tropopause temperature is primarily related to sea surface temperature and ozone. The change in tropopause temperature trend near the year 2000 is related to the change in the sign of the ozone trend with the sea surface temperature having an increased role after 2040. A conceptual model is used to estimate tropopause changes. The results confirm the regression analysis in showing the importance of upper tropospheric warming (connected with sea surface temperature) and stratospheric cooling (connected with CO_2 and O_3). In the past, global warming and ozone depletion have opposite effects on the tropopause temperature, which decreases slightly. For the future simulation, global warming and ozone recovery reinforce which increases the tropopause temperature. In particular, future tropopause change is found not to be an indicator of climate change alone.

1. Introduction

[2] The tropopause is an important region of the atmosphere, which has been traditionally thought of as separating the underlying troposphere from the stratosphere. In recent years the tropopause region has been reconsidered as an individual layer of the atmosphere with its own significance, the tropopause layer [*Birner*, 2006], developing ideas from several decades ago [e.g., *Atticks and Robinson*, 1983]. The tropopause temperature controls the concentration of water vapor which contributes to the chemistry of the stratosphere by providing OH radicals to react catalytically with O_3. H_2O is also an important contributor to the radiative budget of the lower stratosphere [*Forster and Shine*, 2002]. Tropical upwelling has been shown to be anticorrelated with tropopause temperature [*Randel et al.*, 2006]. Therefore in the tropopause layer, dynamics, chemistry, and radiation are interacting and numerical models which include all these processes can provide important insights into tropopause behavior.

[3] In recent modeling studies, S.-W. Son et al. (The tropopause in the 21st century as simulated by stratosphere resolving chemistry-climate models, submitted to Journal of Climate, 2008) and *Gettelman et al.* [2008] intercompared tropopause height and pressure using stratosphere resolving, coupled chemistry climate models (CCMs) as well as models with a limited upper boundary from the Intergovernmental Panel on Climate Change (IPCC) 4th Assessment Report (AR4). It was found that modeled tropopause pressure decreased in the past and in the simulations continues to decrease in the future but at a lower rate. The results also supported earlier work [*Santer et al.*, 2003] which demonstrated that ozone played an important role in the past tropopause trends.

[4] Identifying the reasons for tropopause trends in a model is not straightforward because of the many coupled processes present. As well as the more direct radiative and dynamical processes contributing, as indicated above, sea surface temperatures (SSTs) contribute indirectly by changing the tropospheric and stratospheric circulations [*Schnadt and Dameris*, 2003]. *Fomichev et al.* [2007] also found that an increase in SSTs resulted in a tropopause height increase in a CCM simulation.

[1]Geophysical Fluid Dynamics Laboratory, UCAR, NOAA, Princeton, New Jersey, USA.
[2]Department of Meteorology, University of Utah, Salt Lake City, Utah, USA.

Table 1. Brief Description of Model Simulations

Experiment	Description	Duration
SL1960	Time slice 1960 conditions	30 years
TRANSA	Transient 1960–2005 Initialized year 10 of SL1960	45 years
TRANSB	Transient 1960–2005 Initialized year 20 of SL1960	45 years
TRANSC	Transient 1960–2005 Initialized year 30 of SL1960	45 years
FUTURA	Transient 1990–2100 Initialized year 30 of TRANSA	110 years
FUTURB	Transient 1990–2100 Initialized year 30 of TRANSB	110 years
FUTURC	Transient 1990–2100 Initialized year 30 of TRANSC	110 years

[5] A number of studies have investigated tropopause trends and variations from observations [e.g., *Seidel et al.*, 2001; *Seidel and Randel*, 2006; *Rosenlof and Reid*, 2008]. Satellite data do not have sufficient vertical resolution to be able to detect the very small changes which have occurred and therefore the aforementioned analyses rely on the use of radiosondes. It is also now clear that radiosonde data need to be corrected for trend calculations [*Seidel and Randel*, 2006]. Of these studies, the latter work has demonstrated clear evidence of an increase in tropopause height with a decrease in tropopause temperature and pressure since 1980.

[6] In addition to these studies which also explore the impact of different processes on the tropopause, via observational and modeling methods, a conceptual model of the tropopause [*Shepherd*, 2002] summarizes the general physical processes which influence it. In particular the conceptual model suggests that tropospheric warming increases the tropopause temperature and height and that stratospheric cooling reduces the tropopause temperature and increases the tropopause height. Similar results have been shown in general circulation model experiments of *Thuburn and Craig* [2000].

[7] In this paper we investigate the cold point tropopause in simulations of the Atmospheric Model with Transport and Chemistry (AMTRAC), the Geophysical Fluid Dynamics Laboratory (GFDL) climate model with coupled stratospheric chemistry. The long-term changes are compared with observations for the recent past. The importance of different terms in controlling the long-term change in the tropopause is investigated using multilinear regression. The terms used are among those suggested in the literature as having an impact on the tropopause, adapted toward diagnostics which are readily obtainable from the simulations. The results of the simulations of the model are also compared with the expectations of the conceptual model of *Shepherd* [2002], as well as observations for the recent past. This is used to provide a physical interpretation of the regression analysis.

2. Model Simulations

[8] AMTRAC is described by *Austin and Wilson* [2006] and is a combination of the GFDL AM2 climate model [*Anderson et al.*, 2004] with chemistry from UMETRAC [*Austin and Butchart*, 2003]. The chemistry module is a comprehensive stratospheric scheme with simplified tropospheric chemistry and is fully coupled to the climate model.

The model resolution is 2° by 2.5° with 48 levels from 0.0017 hPa to the ground. The vertical grid spacing decreases steadily from the top of the atmosphere to the surface. In the upper stratosphere it is about 4 km, decreasing to 1.2 km at 100 hPa. The nonorographic gravity wave forcing scheme due to *Alexander and Dunkerton* [1999] is included in the model.

[9] The model simulations used in this study have all been presented in previous work [*Austin and Wilson*, 2006; *Li et al.*, 2008] and are described in Table 1. These consist of a time slice run and transient runs. In the case of the time slice run, the external forcings were kept fixed at values specific to 1960. In the transient simulations, the forcings were varied from one year to the next in accordance with observations or future scenarios.

[10] The time slice run (SL1960) was completed, among other reasons, to provide a range of initial conditions for the transient simulations. The run used monthly varying mean sea surface temperatures (SSTs) and sea ice amounts from a 1960 to 2000 climatology. The greenhouse gas (GHG) and chlorofluorocarbon (CFC) concentrations were set to 1960 values. The solar cycle was not present in the forcings, with radiative and photolysis rates computed using solar mean output. Volcanic aerosol amounts were set to background levels, corresponding to a mean for the years 1996–1998.

[11] Three transient runs for the past were completed (TRANSA, TRANSB, TRANSC). For these, the model was forced with the same time-dependent prescription of GHG and CFC concentrations, tropospheric and volcanic aerosols, and the solar cycle as in the work of *Delworth et al.* [2006] and *Knutson et al.* [2006]. The SSTs were taken from observations (J. Hurrell, personal communication, 2005), extended to the beginning of the year 2005.

[12] Three future runs were completed (FUTURA, FUTURB, FUTURC), and the GHGs were specified from the IPCC scenario A1B [*Intergovernmental Panel on Climate Change*, 2001, Appendix II]. CFC and halon concentrations were taken from chapter 1 and Reference profile A1 in the work of *World Meteorological Organization (WMO)* [2003]. Prior to 1997 the volcanic aerosol amounts were taken from observations. From 1997 onward, the volcanic aerosol optical depths were set constant and equal to the observations averaged over the period 1996 to 1998. SSTs for all three members were taken from a coupled atmosphere-ocean model simulation of the same core climate model, but with fewer vertical levels (simulation CM2.1 of *Delworth et al.* [2006]).

[13] The past runs were initialized from years 10, 20, and 30 of the 1960 time slice run. Unfortunately, because of different volcanic aerosol amounts and differences in the amount of solar forcing, the past runs still needed a few years to spin up to a state in which the changes were responding on climate timescales, rather than on shorter timescales. The future runs were initialized from 1 January 1990 of the corresponding past run. A 15 year overlap between the past and future runs was set up to test the impact of the switch in SSTs from observation to model results. Of all the diagnostics examined in the model, the only noticeable impact was on the ozone hole, which was slightly smaller in the past runs than in the future runs.

[14] For the purposes of analysis, the two runs TRANSA/ FUTURA were here combined into a single run for 1960–
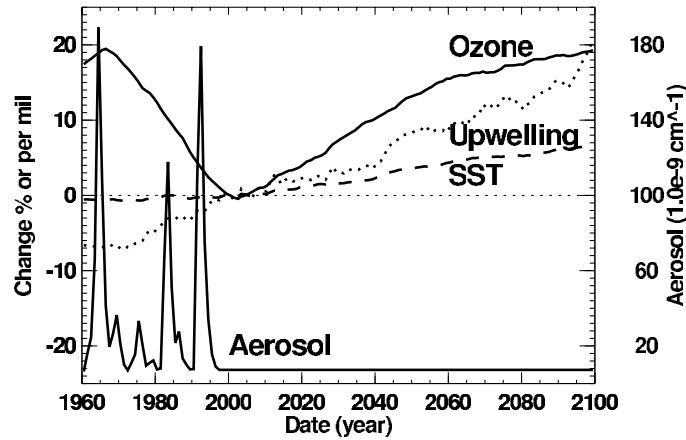
Figure 1. Time series of the independent parameters for the linear regression. The upwelling is given by the thick dotted line to distinguish more easily from the other curves. Ozone and upwelling are given as a percentage change relative to the year 2000. The SST is given in per mil relative to the year 2000. These functions use the left ordinate. The volcanic aerosol term is given in absolute terms and the values are indicated on the right ordinate. The thin dotted line is the zero change line. Annual mean values of the independent variables were used in the regression analysis (equation (1)) but for clarity, except for the volcanic aerosol, 11 year running means have been plotted.

2100, with the results from 1990 onward taken from FUTURA. Similarly for TRANSB/FUTURB and TRANSC/FUTURC. Hereafter, for brevity these combined simulations are referred to as FUTURA, FUTURB, and FUTURC.

3. Analysis Methods

[15] In this section, we describe the method of obtaining the tropopause results and the linear regression model that is used to analyze them. The purpose of the linear regression is to obtain a small set of parameters which can fit the tropopause results to a good approximation. This is then used, together with a conceptual model of the tropopause (section 7), to provide insight in to the physical processes determining the evolution in the tropopause parameters. The independent parameters of the regression have been selected from those suggested in the literature and are suitably adjusted to be readily computed from typical model output.

3.1. Calculation of Cold Point Tropopause Values

[16] The tropopause values were calculated following the method of *Reichler et al.* [2003] using the full three-dimensional temperature fields at daily intervals. This method uses vertical interpolation to calculate tropopause pressure and temperature from gridded fields with coarse vertical resolution. In contrast to the standard World Meteorological Organization definition [*WMO*, 1957], here the vertical interpolation determines the location of the minimum temperature or the cold point tropopause. Using daily fields of surface pressure as additional input, the hypsometric equation was then integrated from the surface to the tropopause pressure to determine the geometric height of the tropopause.

[17] The tropopause data were further averaged zonally over the model grid points from 22°S to 22°N, which are closest to the tropics, to yield a time series of tropical tropopause data for each day of the approximately 500 years

of simulations. Daily values were then averaged to give annual values. By determining the tropopause parameters first and then averaging the results, in principle the errors in determining the tropopause trends are reduced.

3.2. Linear Regression Model

[18] The annually averaged tropopause temperature, pressure, and height data for the years 1960 to 2099 were fitted to the following regression equation:

$$A(t) = a_0 + a_1 s + a_2 SST + a_3 \Omega + a_4 M_F + \varepsilon(t) \qquad (1)$$

where $A(t)$ is the annually averaged model quantity, t is time in years, s is the volcanic aerosol surface area at 60 hPa at the equator estimated from the optical depth [*Thomason and Poole*, 1997], SST is the sea surface temperature averaged zonally from 22°S to 22°N, Ω is the globally averaged total ozone column, and M_F is the tropical mass upwelling at 77 hPa, $2\pi a^2 \int_{\theta_S}^{\theta_N} \rho \overline{w}^* cos(\theta) d\theta$, where a is the radius of the Earth, and ρ is air density. Here θ_N and θ_S are the latitudes in the north and south, where the residual vertical velocity, $\overline{w}^*$ changes from upward to downward, the "turnaround latitudes." This is the same calculation as used by *Butchart and Scaife* [2001], who instead used model output from the 68 hPa level. The residual term, $\varepsilon(t)$, is taken to be first-order autoregressive using the method of *Tiao et al.* [1990].

[19] After detrending all the terms to transform them to approximately stationary variables, equation (1) was solved for the coefficients a_i, using the least squares algorithm developed for the Numerical Algorithms Group Fortran library [*Numerical Algorithms Group*, 1999]. The algorithdm also provided standard statistical uncertainties for the different terms. These uncertainties for the model temperature are discussed in section 5. This method proved to be ineffective for addressing the long-term trends in tropopause temperature, and so the calculations were repeated with the trends included in each of the
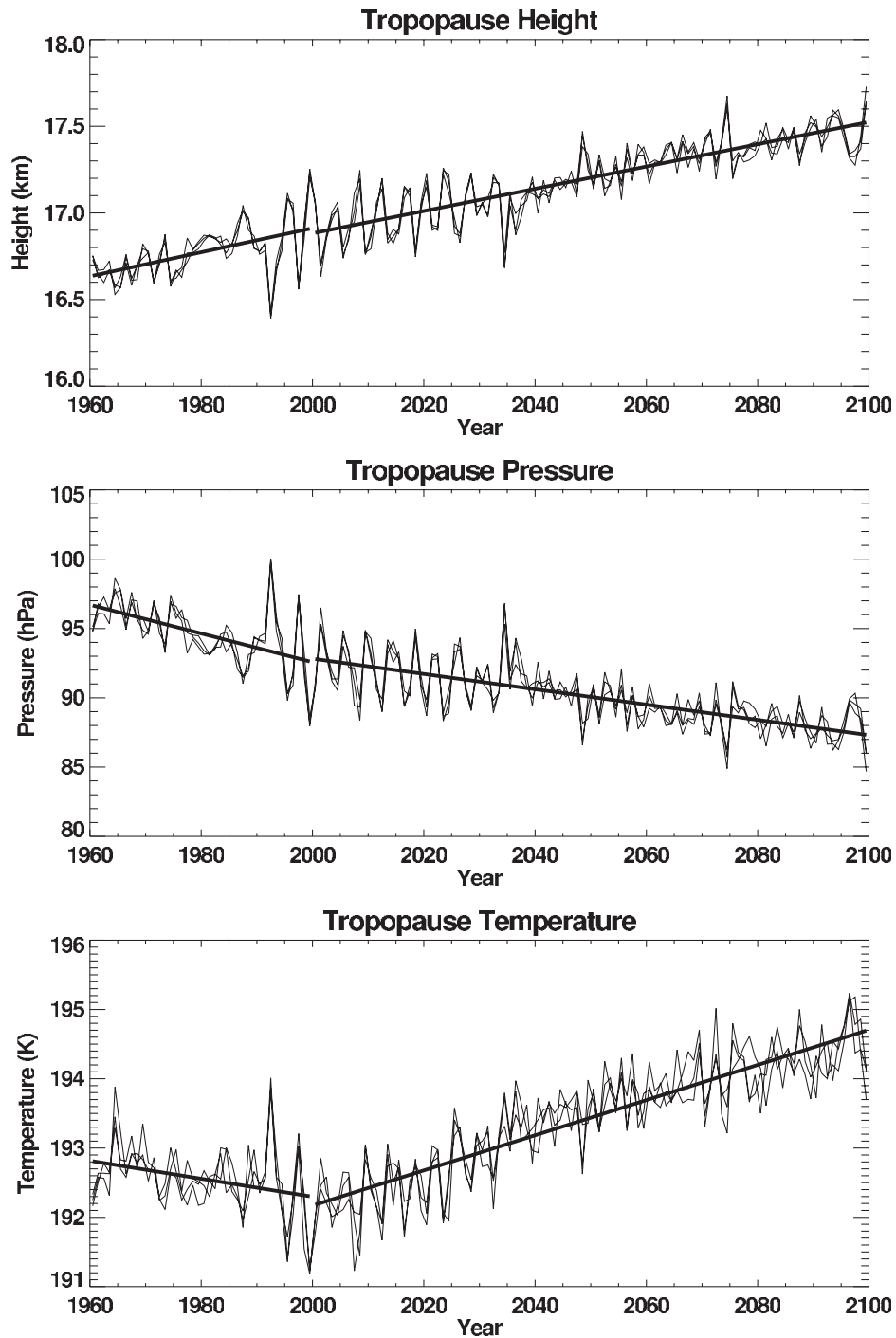
Figure 2. Height, pressure, and temperature of the cold point tropopause, averaged over the tropics. The thin lines are the results from the individual experiments. The thick black lines are linear regression lines through the ensemble mean data.

terms. The contrast in results obtained with these different methods is discussed in section 5.

3.3. Choice of Independent Parameters for the Regression

[20] The choice of independent parameters in the regression is to some extent arbitrary and is here discussed further. First, equation (1) represents the major processes known to

influence the tropopause, as mentioned in section 1, including volcanic aerosol loading, SSTs, ozone, and vertical motion. Time series of the independent terms in the regression analysis are shown in Figure 1 for the 140 year period.

[21] The aerosol loading used here is a zonal average at a specific pressure in the lower stratosphere. This pressure is chosen since it is likely that volcanic aerosol primarily

Table 2. Linear Trends in the Tropopause Temperature, Pressure, and Height for Different Periods Averaged for All Three Experiments[a]

Quantity	Tropics 1960–1999	Tropics 2000–2099	Global 1980–2004	Global Observations
Temperature	−0.130 ± 0.069	0.254 ± 0.014	−0.27 ± 0.06	−0.41 ± 0.09
Pressure	−1.03 ± 0.30	−0.55 ± 0.06	−2.6 ± 0.4	−1.7 ± 0.6
Height	70 ± 22	64 ± 5	123 ± 18	64 ± 21

[a]Temperature is measured in K/decade, pressure is measured in hPa/decade, height is measured in m/decade. Error bars are 2σ uncertainties and observations are from *Seidel and Randel* [2006].

affects the lower stratosphere. Other possibilities would have been to use a vertically integrated term. This is not explored further, as the aerosol has a small impact on the results (section 5).

[22] An SST term has been included because of the expected dependence of the tropopause on sea surface temperatures [e.g., *Fomichev et al.*, 2007; *Rosenlof and Reid*, 2008]. Year to year changes will be dominated by the presence of El Niño, and hence an El Niño index might have been used. Instead we use a simple tropical mean as this is easy to compute for the future simulations. Climate change will have a direct impact on the mean SST and this is commented upon later. An El Niño index would likely reveal a different relationship with the tropical tropopause data, depending on the relationship between climate change and El Niño. This particular issue is beyond the scope of the current work.

[23] Stratospheric ozone may have an impact on the tropopause via the radiative heating [e.g., *Seidel and Randel*, 2006]. The ozone term used here is the global average total column. Again, many other ozone diagnostics may be relevant including more local measures. However, it is here suggested that the ozone concentration outside the tropics affects the tropopause temperature because of its influence on the stratospheric general circulation, and this may be generally represented by the ozone global average. Despite this argument, repeating the calculations using tropical ozone in equation (1) instead of global ozone yielded virtually identical results. Naturally, the column amount contains a tropospheric component, but its variability and trend are considerably smaller than the stratospheric component. The total column is also a convenient term to use, rather than for example the stratospheric column, because the total column is readily available from observations and in the model diagnostics that are typically produced.

[24] An impact of the Brewer-Dobson circulation on tropical tropopause temperatures was indicated by *Yulaeva et al.* [1994] and *Randel et al.* [2006]. This is represented by the tropical mass upwelling which was shown by *Butchart and Scaife* [2001] and *Butchart et al.* [2006] to be a robust measure of the strength of the Brewer-Dobson circulation. The quantity is here computed for the lower stratosphere (77 hPa) and integrated over the range of latitudes, which vary seasonally, where the circulation is upward. The quantity is robust in the sense that despite large interannual variability, over climate timescales it has been shown to increase in a large number of climate model simulations, with and without chemistry [*Butchart et al.*, 2006] and therefore SSTs and upwelling may not be entirely independent parameters. Furthermore, the inclusion of this term provides a useful connection between tropopause

properties and broad stratospheric transport properties such as the age of air [*Austin and Li*, 2006]. Upwelling also depends to some extent on the ozone trend [*Li et al.*, 2008] but we have included all three terms (in addition to aerosols) in order to determined their relative weight and importance for the tropopause parameters.

4. Model Tropopause Results

[25] The height, pressure, and temperature of the tropopause are shown for the three experiments in Figure 2. The interannual variation is very similar in each simulation indicating that external forcing such as the volcanic aerosol amount or the SST are likely to be responsible as these are common to all three simulations. For example, the peaks in temperature in 1964 and 1992 coincide with high aerosol following the eruptions of Agung and Mt. Pinatubo. For all three quantities the rate of change was significantly different from zero at the 95% confidence level. In the following, the error bars are 2σ uncertainty intervals and have been determined from the least squares fit (see Table 2). The effect of systematic processes such as the above eruptions is to increase the computed uncertainty for the past trend but also to increase the trend during the volcanic years. In addition to tropical values, the trends were also computed globally for the period 1980 to 2004 to compare directly with the observations of *Seidel and Randel* [2006], which we favor as the best assessment of tropopause trends. However, it is clear from their paper that there are considerable uncertainties in estimating tropopause trends from observations, due to issues such as instrument drift and bias, as well as the nonuniform global coverage. Analyses from data assimilation in principle provide uniform coverage, and some results from this source are cited here [e.g., *Santer et al.*, 2004]. Nonetheless, data assimilation fields are not designed for trends, as there is not necessarily an attempt to correct instruments for data bias prior to insertion in the analysis, and the instrument mix typically changes over the multidecadal time frame that is relevant [e.g., *Rood*, 2005].

[26] The tropical tropopause height (Figure 2, top) increased with little long-term variation, 70 ± 22 in the past compared with 64 ± 5 m/decade in the future. For the full 140 year period, the trend in the tropopause height was 63 ± 3 m/decade. In the global average since 1980, the trend was somewhat larger at 123 ± 18 and about twice the observed value of 64 ± 21 m/decade [*Seidel and Randel*, 2006].

[27] In contrast to the height, the tropical tropopause pressure (Figure 2, middle) showed a significant difference between the past, when it decreased at about 1 hPa/decade, and the future, when it decreased at about half the rate. This is consistent with the results shown by Son et al. (submitted
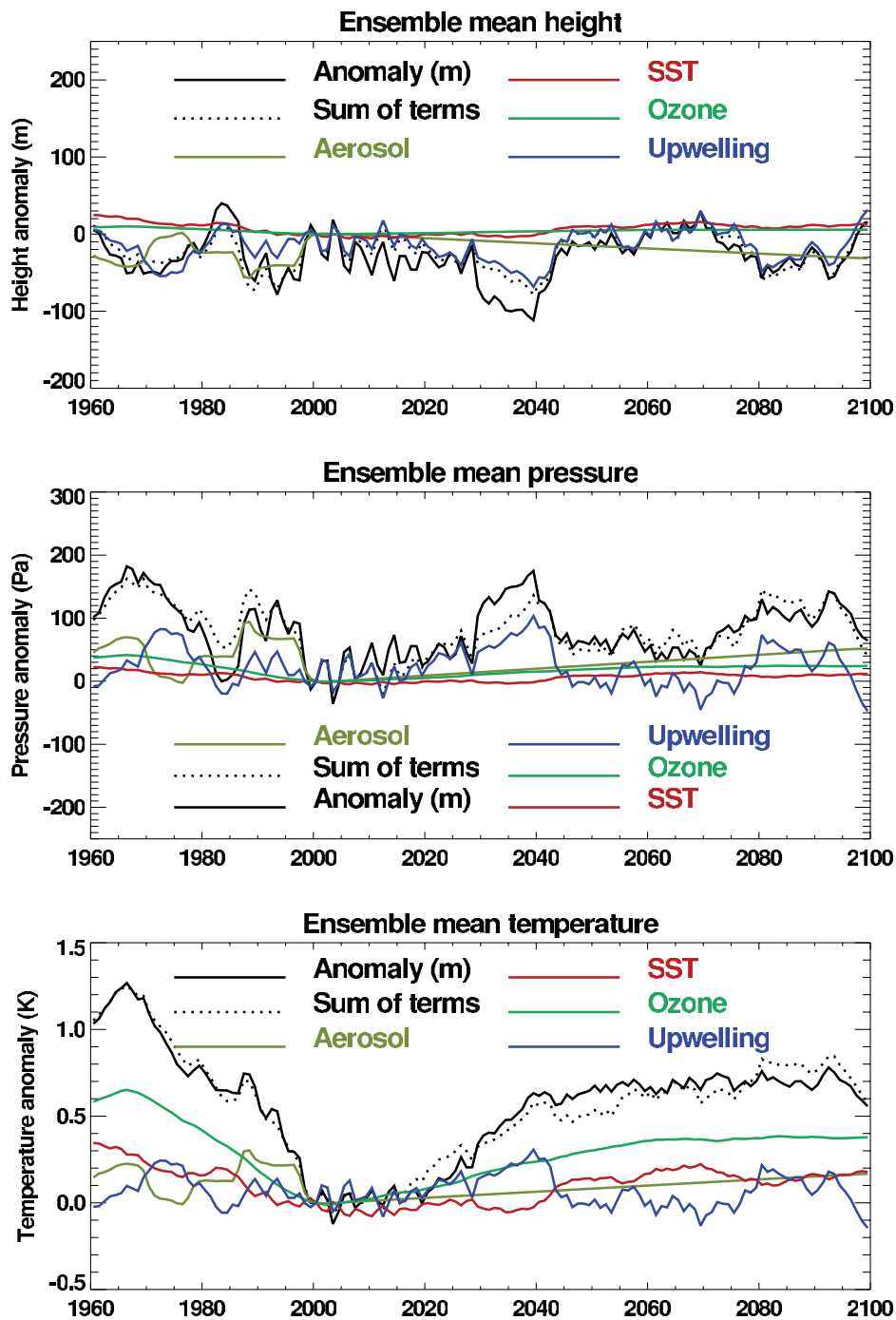
Figure 3. (top) Contribution of each of the terms in the linear regression analysis of the detrended tropopause height. The sum of the terms is shown by the dotted black line, which may be compared with the tropopause height (solid black line). The regression model was applied to the annual mean fields with the mean trends for the period 1960–2100 removed, and ensemble mean, 11 year running averages are shown. The values plotted are relative to the year 2000. (middle) As in Figure 3 (top) but for tropopause pressure. (bottom) Tropopause temperature.

manuscript, 2008) and *Gettelman et al.* [2008] for our model. The global average trend since 1980 is larger than observed [*Seidel and Randel*, 2006], although the error bars overlap. In comparison the model result is close to the trend derived by *Santer et al.* [2004] from reanalysis data, -2.5 ± 0.5 hPa/decade.

[28] Overall, the tropopause temperature is biased low compared with observations by about 4 K [*Eyring et al.*, 2006], but this bias is considered unlikely to affect substantially the processes which determine the trends. The most dramatic change in trend occurred in the tropopause temperature (Figure 2, bottom), which decreased significantly

Table 3. Regression Coefficients for the Tropopause Temperature With Uncertainties Given As One Standard Error Computed From the Regression Analysis Using Detrended Data[a]

	Coefficient a_i			
Term	A	B	C	Mean
Constant	0.00 ± 0.23	0.00 ± 0.23	0.00 ± 0.26	0.00 ± 0.29
SST	0.666 ± 0.002	0.664 ± 0.002	0.665 ± 0.002	0.656 ± 0.002
Column ozone	1.17 ± 0.13	1.25 ± 0.13	1.09 ± 0.15	1.19 ± 0.17
Mass upwelling	-1.41 ± 0.064	-1.34 ± 0.050	-1.34 ± 0.057	-1.05 ± 0.049
Volcanic aerosol	0.65 ± 0.08	0.68 ± 0.07	0.68 ± 0.08	0.66 ± 0.07

[a]Units are K, K/K, K/100DU, $K/10^9$ kg m^{-2} s^{-1}, and $K/10^{-6}$ cm^2/cm^3 for the constant, SST, column ozone, upwelling, and aerosol terms, respectively. Values are given for the individual experiments (A, B, C) and for the results in which the regression is applied to the ensemble mean data.

in the past simulation at a rate of 0.13 K/decade and increased significantly in the future simulation at about twice the rate. The model trend in the global average since 1980 is −0.27 K/decade which is smaller than the trend estimated from observations, −0.41 K/decade [*Seidel and Randel*, 2006], although the error bars overlap.

5. Results of the Regression Analysis

5.1. Detrended Results

[29] The contributions of the individual terms in the regression analysis for the tropopause height, pressure, and temperature are shown in Figure 3. Also shown in Figure 3 are the model tropopause terms from Figure 2, after detrending the data, and the sum of the terms in the regression analysis. Values were computed separately for each experiment using annual average data. The values for the individual experiments were very similar, and so only the ensemble mean values are shown. For clarity all the values in Figure 3 have been smoothed with an 11-year running mean.

[30] Although most of the individual terms of equation (1) have only a small impact, the tropopause height is clearly correlated with M_F, the mass upwelling on the constant pressure surface of 77 hPa. In the three experiments the upwelling regression coefficients obtained were 308 ± 20, 307 ± 16, and 300 ± 18 (in units of $m/10^9$ $kgm^{-2}s^{-1}$).

[31] The results for tropopause pressure are almost a mirror image of the results for height, although there are some important differences which are explored in section 6. The tropopause pressure is clearly anticorrelated with the mass upwelling and the regression coefficients for the three experiments were -464 ± 26, -464 ± 20, and -455 ± 24 $Pa/10^9$ $kgm^{-2}s^{-1}$. Figure 3 shows that the upwelling term is very well correlated or anticorrelated with height and pressure changes on both short (interannual) and very long (multidecadal) timescales, but SSTs do not exhibit a relationship with height or pressure.

[32] The results for tropopause temperature are very different in indicating that several terms are important. The main contributing term was ozone throughout the period, but each of the other terms provided important contributions, particularly the upwelling as indicated in the last decade. The regression coefficients for the three experiments are given in Table 3. We note in particular that the individual experiments are consistent with each other, and, furthermore, the upwelling is anticorrelated with temperature, in accordance with previous findings [e.g., *Randel*

et al., 2006]. In section 5.2, we find that this anticorrelation can be misleading in the application to climate timescales.

5.2. Application of the Results to the Long-Term Variability

[33] Figure 4 shows the results obtained after applying the regression coefficients in Table 3 to the long-term varying data. This is equivalent to adding, to the results shown in Figure 3, the terms $(t-2000)$ a_i $\dot{x}_i$ where $\dot{x}_i$ is the long-term trend of each of the independent variables. For height and pressure, the regression fit is very good when all the terms are considered in the regression. The root mean square deviation of the linear regression from the ensemble model tropopause height and pressure are only 26 m and 31 Pa compared with a total change of 850 m and 900 Pa during the simulations. In contrast the fit for temperature is poor, indicating that different processes are operating on the long timescale than on the short timescale revealed by the detrended data.

[34] A partial explanation for this result is indicated in Figure 5, which shows the correlation coefficient between the annually varying tropopause data and the annually varying ozone, SST, and upwelling terms. The coefficient is computed as a function of the period length, averaged over the available periods. Thus results for timescale n years are computed from the $140/n$ separate periods. The results show that for SST and upwelling, and to a lesser extent ozone, short periods give rise to an anticorrelation with tropopause temperature, whereas long timescales give a positive correlation. The results for the detrended data are shown by the dotted lines in Figure 5. These give a very different picture indicating that much of the long timescale variation in SSTs and upwelling arise from the linear trend. Essentially, for the longer timescales the variance due to climate change starts to exceed the variance due to interannual variability and the regression reflects climate processes. This is discussed further in section 8.

[35] A good fit to the temperature data can be recovered by first including the long-term trends in the data and then smoothing the independent data before repeating the regression analysis. These results are shown in Figure 6 and the individual regression coefficients obtained are given in Table 4. Also shown in Table 4 are the cumulative variances explained by the inclusion of the terms in the regression for the past and for the whole period of the simulations.

[36] Unlike in the cases of tropopause pressure and height, many of the individual forcing terms have important contributions at different times. For all three experiments,
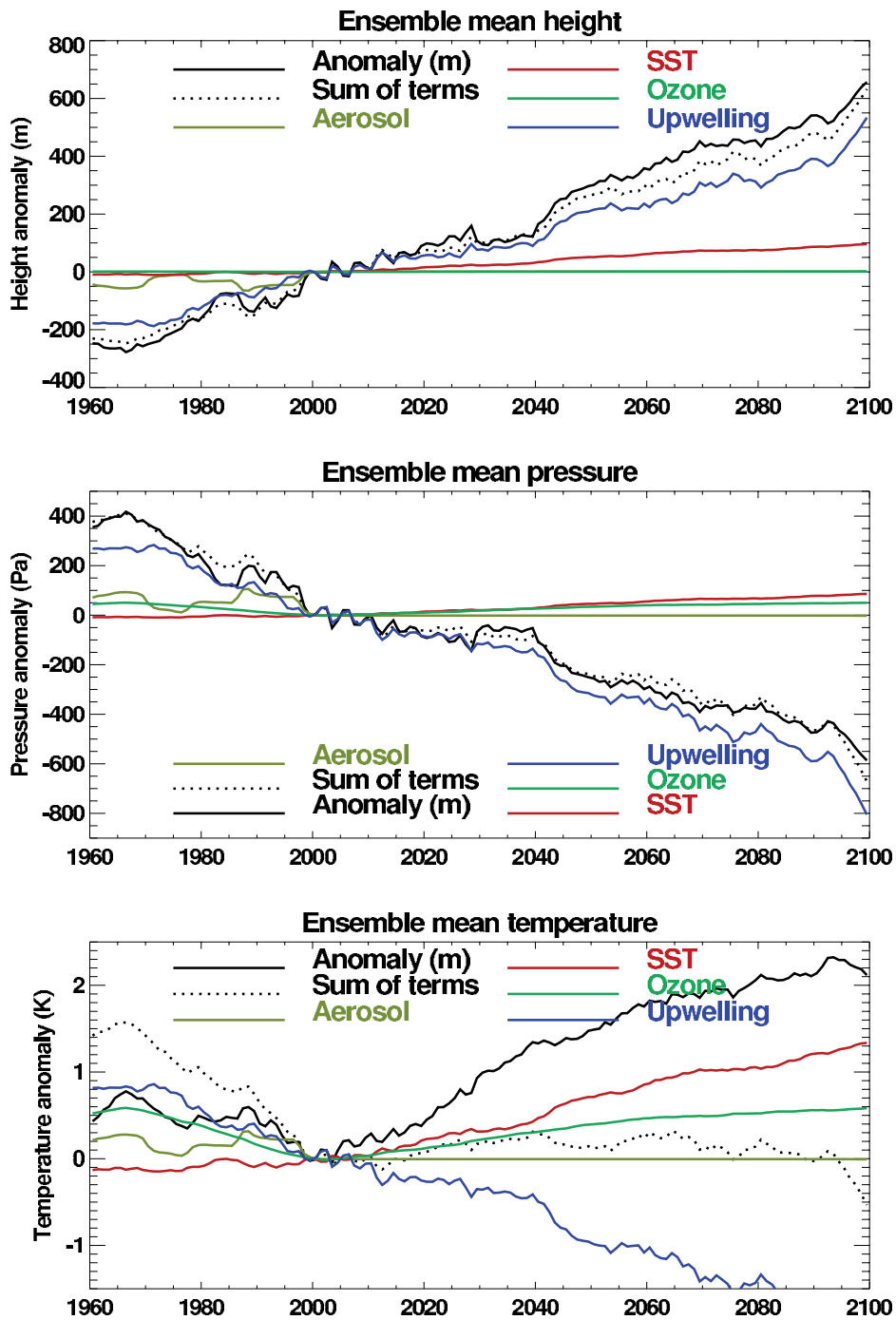
Figure 4. As in Figure 3, after applying the same regression coefficients, to the long-term varying data.

the results are very similar and only the ensemble means are shown. In the past, the temperature broadly follows the ozone term and indeed this is confirmed by the regression which indicates that ozone is the dominant factor, contributing about 30% of the variance. The other terms are much smaller and tend to have opposite effects, with each term supplying about 15% of the variance or less. After 2000, the ozone term increases linearly at first but from from about 2050 tends to approach a steady value corresponding to chlorine in the atmosphere having returned to pre-1980 values. By contrast the SSTs continue to increase and the two terms together provide a large part of the variance. The

upwelling term also increases during this time and the details of the tropopause temperature follow from a combination of these three terms. In particular the non uniform trend in tropopause temperature follows from the reduction in ozone trend in the latter half of the 21st century.

[37] For the period as a whole, the SST term is dominant, contributing 80% of the variance, with ozone contributing about 14%, and the upwelling having a minor role. As seen in Figure 6, the SST term starts to dominate ozone after about 2040. The volcanic aerosol effect is quite small because of the effect of the decadal averaging. Although the term contributes about 15% to the variance of the
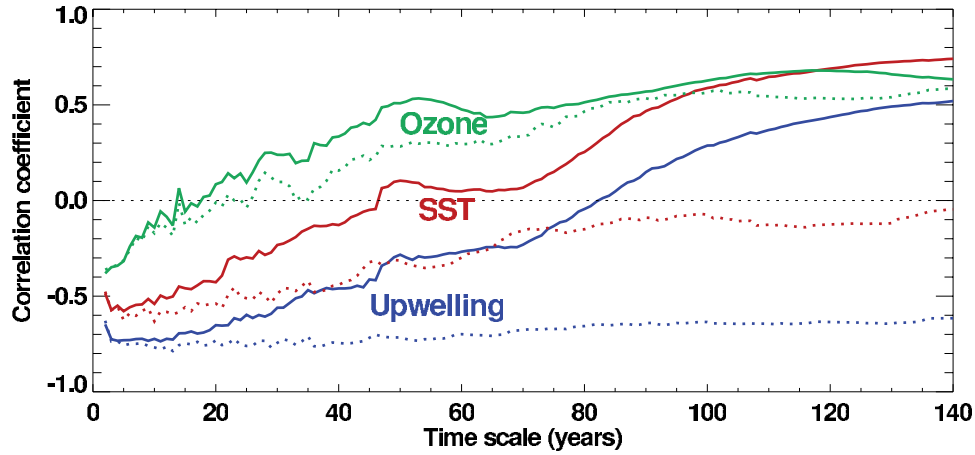
Figure 5. Correlation coefficient between annually averaged tropopause temperature and three of the independent forcing terms in the regression. The other two processes involving aerosols and the solar cycle were generally small and have not been included. Results are presented as a function of timescale by dividing the 140 year time series in to $140/n$ periods of length n years. Calculations were performed for each of the three model simulations and the mean regressions are plotted. The dotted lines are the results obtained for the detrended data.

tropopause temperature for the past, it is negligible in the full run since the aerosol is fixed after 1997. The sum of the individual terms agrees with the decadally averaged tropopause temperature to within 0.12 K root mean square compared with a change of 2.1 K from 2000 to 2100.

6. Relationship Between Height, Pressure, and Temperature Changes

[38] Some further insights in to the reasons for the changes in trends near the year 2000 shown in Figure 1 can be obtained by examining the relationship between the height and pressure of the tropopause. The height of the tropopause at different times is given by

$$z_{t1} = \int_{p_{t1}}^{p_s} dp/g\rho_1 \qquad\qquad z_{t2} = \int_{p_{t2}}^{p_s} dp/g\rho_2 \qquad (2)$$

z_{t1} and z_{t2} are the heights at the two times and p_{t1} and p_{t2} are the corresponding pressures. The variables ρ_1 and ρ_2 are the

tropospheric air density profiles and p_s is surface pressure. The difference in heights is given by:

$$z_{t1} - z_{t2} = \int_{p_s}^{p_{t1}} \frac{dp}{g}\left(\frac{1}{\rho_1} - \frac{1}{\rho_2}\right) - \int_{p_{t2}}^{p_{t1}} \frac{dp}{g\rho_2} \qquad (3)$$

Using the gas equation $p = \rho\,RT$, where R is the gas constant and T is temperature, we obtain:

$$z_{t1} - z_{t2} = \frac{R}{g}\int_{p_s}^{p_{t1}} (T_1 - T_2)\frac{dp}{p} - \frac{R}{g}\int_{p_{t1}}^{p_{t2}} T_2\frac{dp}{p} \qquad (4)$$

The right-hand terms of equation (4) were computed numerically from the complete model output and the results are shown in Figure 7. Also, $T_2 = \overline{T}$ is approximately
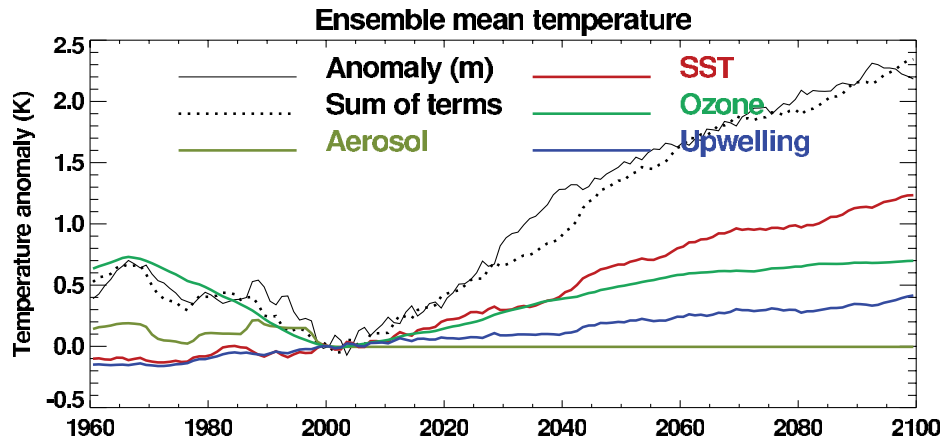

Figure 6. Contribution of each of the terms in the linear regression analysis of the tropopause temperature for the ensemble mean of the simulations. The regression model was applied to the data which were smoothed with an 11 year running mean.

Table 4. As in Table 3 but Using the Time Varying Fields in the Regression Analysis Without Detrending[a]

| Term | Coefficient a_i | | | | % Variance | Explained |
	A	B	C	Mean	1960–1999	1960–2099
Constant	0.00 ± 0.47	0.00 ± 0.47	0.00 ± 0.43	0.00 ± 0.42	0.0	0.0
SST	0.620 ± 0.004	0.619 ± 0.004	0.621 ± 0.004	0.620 ± 0.003	0.0	80.3
Column ozone	1.51 ± 0.31	1.62 ± 0.30	1.24 ± 0.28	1.41 ± 0.26	28.7	94.8
Mass upwelling	0.242 ± 0.112	0.263 ± 0.116	0.334 ± 0.111	0.262 ± 0.077	44.5	97.4
Volcanic aerosol	0.41 ± 0.41	0.34 ± 0.41	0.58 ± 0.39	0.34 ± 0.21	61.8	97.9

[a]The cumulative variance of the 11-year smoothed results explained by the independent parameters is included corresponding to the two periods indicated.

constant over the narrow tropopause pressure range and equation (4) becomes:

$$z_{t1} - z_{t2} = \frac{R}{g}\left\{ \int_{p_s}^{p_{t1}} (T_1 - T_2)\frac{dp}{p} - \overline{T}ln(p_{t1}/p_{t2}) \right\} \quad (5)$$

The first term in equations (4) and (5) is essentially the thermal expansion of the troposphere. The second term is the height increase due to what may be considered structural changes in the upper troposphere/lower stratosphere region itself. To a first approximation, $\overline{T}$ can be replaced by the tropopause temperature for the year 2000.

[39] Throughout the integration the sum of the two terms is very close to the tropopause height determined directly. For the 1960–2000 period, the second term of equation (4) is approximately 200 m (50 m/decade). The first term is small since although the surface has been warming slightly, the tropopause has been cooling. In the future, the tropospheric expansion and UTLS change terms are very similar in size. Since for small pressure differences, $ln(p_{t1}/p_{t2}) \simeq (p_{t1} - p_{t2})/p_{t2}$, these results show that for the future in which the tropospheric expansion term is nearly proportional to the UTLS term, the tropopause height trend is approximately linearly related to the tropopause pressure trend. The relationship between the tropopause height trend and the tropopause temperature trend is not clear. Nonetheless, it would be reasonable to suggest that the reduced tropical troposphere expansion for the period 1960 to 2000 is related

by radiative heating to the decrease in stratospheric ozone which in turn contributed to the tropopause temperature as indicated in Figure 6.

7. Conceptual Tropopause Model

[40] Although the regression model was successful in fitting the model tropopause results to a small number of parameters, regression can only indicate possible connections. To establish a physical relationship between given parameters and, in the current case, tropopause model results, we here simplify the problem of the causes of tropopause trends using a conceptual model [Shepherd, 2002]. The expected response of the tropopause to tropospheric warming and stratospheric cooling is schematically depicted in Figure 8.

[41] Using the framework introduced by Shepherd [2002], Staten and Reichler [2008] show that changes in the height of the tropopause Δz_{trop} are given by:

$$\Delta z_{trop} = (\Delta T_t - \Delta T_s)/(\gamma_t - \gamma_s) \quad (6)$$

and changes in tropopause temperature ΔT_{trop} are obtained from

$$\Delta T_{trop} = (\Delta T_s \gamma_t - \Delta T_t \gamma_s)/(\gamma_t - \gamma_s) \quad (7)$$

The variables γ_t and γ_s are the lapse rates ($-\partial T/\partial z$) and ΔT_t and ΔT_s are the temperature changes in the troposphere and
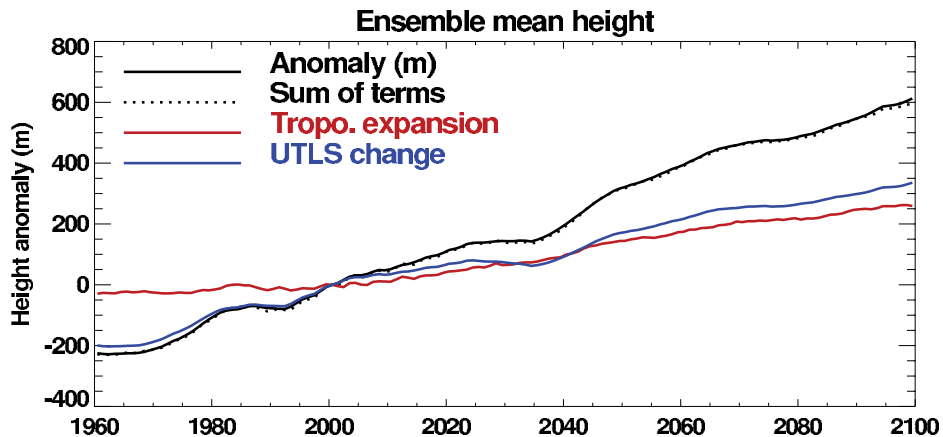

Figure 7. Contribution to the individual terms in the determination of the tropopause height. The tropospheric expansion and UTLS change terms are given by the right-hand side of equation (4). The black solid curve is the tropopause height computed directly and the dotted curve is the sum of the two terms in equation (4). An 11 year running mean has been applied to the results to reduce the effect of interannual variability and the solar cycle.
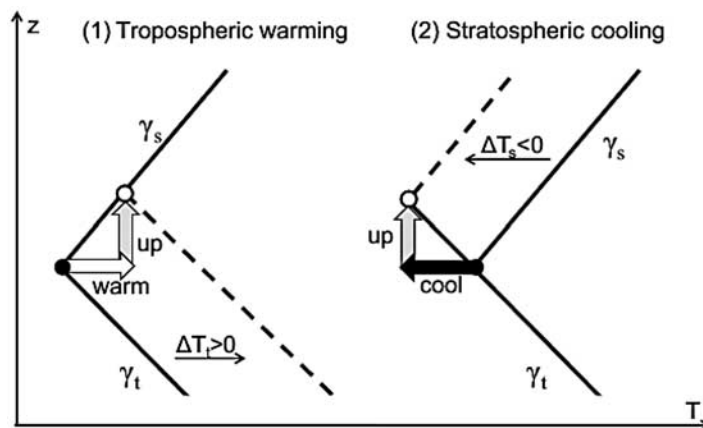
Figure 8. Schematic depiction of tropopause response (arrows) to tropospheric and stratospheric temperature perturbations (dashed lines).

the stratosphere respectively. Thus, the conceptual model assumes no change in lapse rates and determines the tropopause response entirely from the temperature change below and above the tropopause.

7.1. Applicability of the Conceptual Model

[42] The predictions of the conceptual model are examined using values for ΔT_t, ΔT_s, γ_t, and γ_s separately from runs TRANS and FUTUR. The corresponding tropopause trends are diagnosed using equations (6) and (7), and the results are compared with the actual tropopause trends determined from the full model (Table 2). The ΔT and γ values needed for equations (6) and (7) were derived from vertical temperature profiles and their trends, which are indicated by the black lines in Figure 9. The temperature trends of the two simulations are nonuniform in the vertical. For example, in the troposphere both runs exhibit an increase in warming trend with height, a well-known
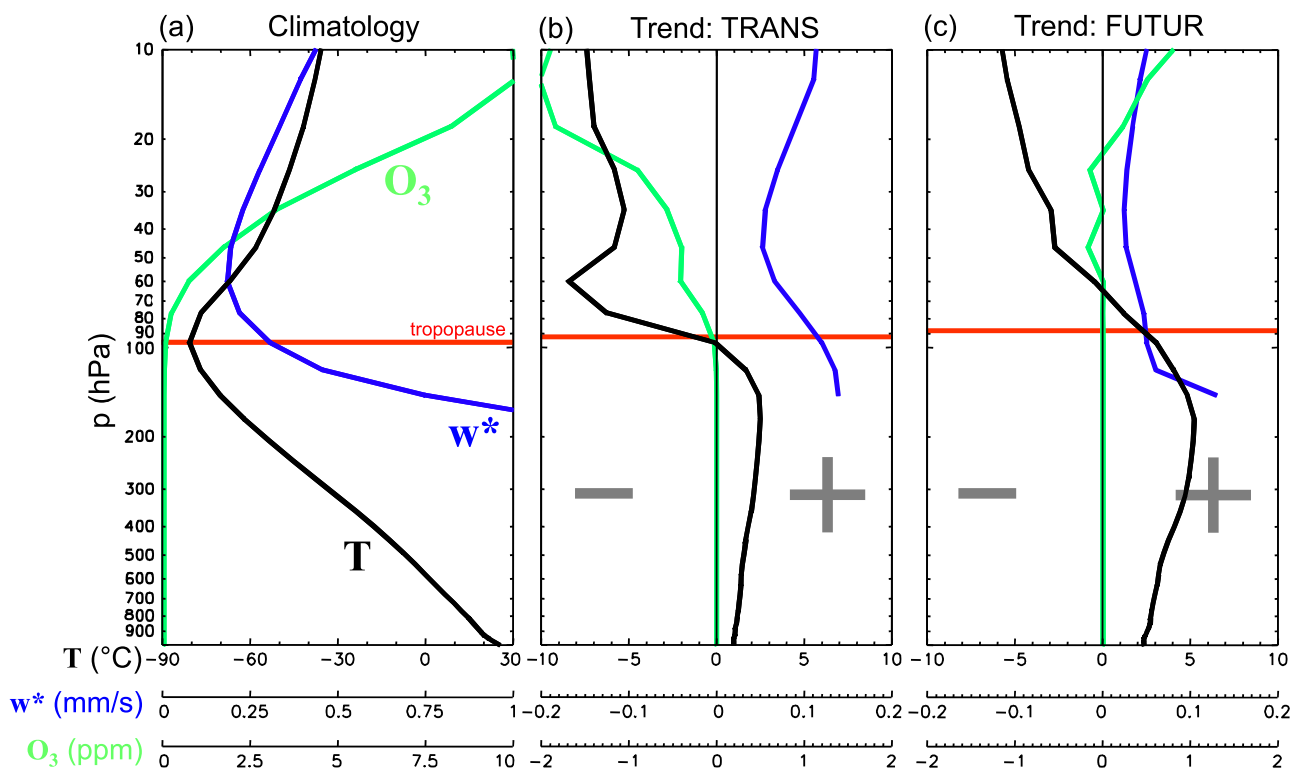

Figure 9. Vertical profiles of temperature T, residual vertical velocity w^*, and ozone mixing ratio O_3 in the tropics, showing (a) the 1960–1969 climatology derived from run TRANS and (b and c) linear trends (per century) for TRANS (1960–1999) and FUTUR (2000–2099), respectively. All data are averages over three ensemble members, over the zonal direction, and from 22°S to 22°N latitude. The horizontal red line denotes the location of the cold point tropopause at the beginning (Figure 9a) and end (Figures 9b and 9c) of the runs.

Table 5. Stratospheric and Tropospheric Temperature Trends Used to Test the Simple Tropopause Model[a]

		TRANS	FUTUR
ΔT_s	zero	0.0	0.0
ΔT_s	LS	−5.0	0.0
ΔT_t	zero	0.0	0.0
ΔT_t	LT	1.0	2.5
ΔT_t	UT	2.5	5.0

[a]Temperature is measured in K/century. The values for the lower troposphere (LT), upper troposphere (UT), and lower stratosphere (LS) are estimates taken from Figure 9.

consequence of the quasi-moist adiabatic adjustment of the atmosphere to global warming. In this analysis it is therefore unclear which values of ΔT_t and ΔT_s to use in the above equations. Several plausible combinations of ΔT values are used and how a particular choice affects the outcome of the tropopause diagnostic is investigated. The chosen values, listed in Table 5, were derived from the temperature trend profiles (Figure 9) at the following levels: The lower troposphere (LT) (approximately 1000 hPa), the upper troposphere (UT) (approximately 200 hPa), and the lower stratosphere (LS) (approximately 70 hPa). The lapse rate changes induced by the temperature trends amount only to a few percent. As pointed out before, the constant lapse rate assumption therefore holds and in all subsequent calculations representative constant climatological mean lapse rates of $\gamma_t = 6 \times 10^{-3}$ Km^{-1} and $\gamma_s = -4 \times 10^{-3}$ Km^{-1} are used.

[43] Figure 10 shows the results of the conceptual model using the above combination of values compared with the actual tropopause changes determined from the full dynamical model. For data from run TRANS (black symbols), considering only lower or upper tropospheric temperature changes (LT or UT) and setting stratospheric temperature

changes to zero leads to quite unrealistic results. The predicted tropopause warms whereas the actual tropopause (ACTUAL) cools. When only lower stratospheric temperature changes are considered (LS) and tropospheric temperature changes are neglected, the prediction is much closer to the actual change. The model prediction is even more realistic when both stratospheric and (lower or upper) tropospheric temperature changes (LT/LS or UT/LS) are included. To first order, however, this suggests that stratospheric temperature changes are most important for the actual tropopause change in run TRANS.

[44] The gray symbols in Figure 10 show the results for run FUTUR. Varying the tropospheric temperature change from zero (LS) to 2.5 (LT/LS) to 5 K per century (UT/LS) shows clearly improved tropopause predictions. Since the LS temperature change is small, zero was used as the best estimate for ΔT_s. Therefore, in this case it is not possible to test the influence of stratospheric temperature change on the prediction of the simple model. In run TRANS, the specification of realistic LS temperature change is crucial, a fact which is clearly related to the large magnitude of the LS temperature change in that run (−5 K per century). To a lesser extent, and as discussed by *Staten and Reichler* [2008], this is also related to the higher sensitivity of the simple tropopause model to stratospheric change. In addition, the results for both runs reveal that upper tropospheric temperature change is the more appropriate ΔT_t parameter as opposed to the temperature change at the surface. This is also to be expected, since UT temperature change includes the effect of changing lapse rate.

[45] We note the good agreement between our study and the results of *Randel et al.* [2003], who find robust relationships between cold point parameters and observed atmospheric temperatures over a narrow range (approxi-
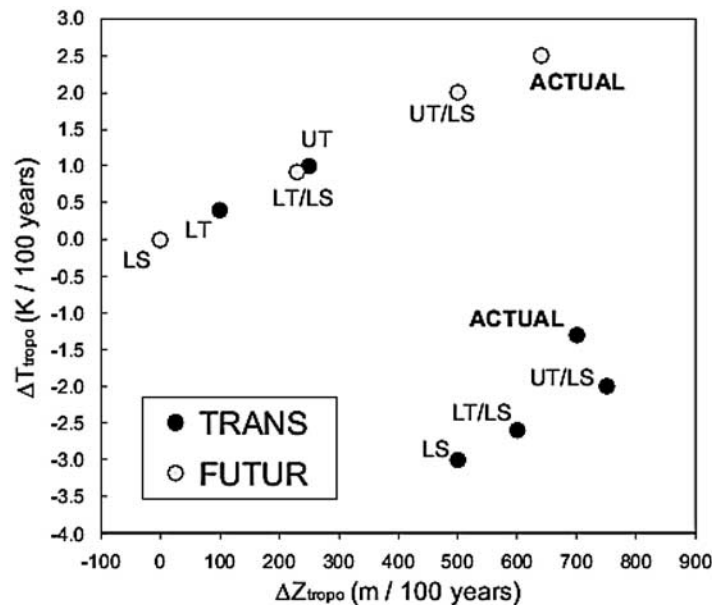

Figure 10. Height (abscissa) and temperature (ordinate) trends (per century) of the tropical cold point tropopause. The trends were either directly determined from the full temperature profiles of the model (ACTUAL) or predicted by the simple tropopause model using different combinations of stratospheric and tropospheric temperature changes. Black symbols denote results from TRANS, and gray symbols are for FUTUR.

mately 1–3 km) above and below the tropopause. For example, cold point temperatures are positively correlated with temperatures above and below, whereas cold point heights are positively correlated with temperatures below and negatively correlated with temperatures above. Cold point heights and temperatures themselves are uncorrelated. These results are consistent with the conceptual model (Figure 8) and indeed confirm that the most appropriate parameters to drive the conceptual model are the temperature trends in the vicinity of the tropopause (UT and LS).

7.2. Attribution Analysis for Tropopause Change

[46] According to the conceptual model, both tropospheric warming and stratospheric cooling lead to an increase in tropopause heights, which agrees well with the very robust height increases seen in the model simulations. In contrast, the temperature responses of the tropopause to the two perturbations below and above are of opposite sign, so that their combined effect depends on the magnitude of the temperature perturbations. Based on the temperature trends shown in Figure 8 and Table 5, in TRANS, strong stratospheric cooling counteracts the smaller tropospheric warming. In FUTUR, by comparison, tropospheric warming is much more pronounced than stratospheric cooling, and the tropopause therefore warms.

[47] The tropospheric warming is clearly due to greenhouse gas related global warming. The stronger warming seen in FUTUR as compared to TRANS is consistent with the larger rate of CO_2 increase (330 ppm per century versus 140 ppm per century). The reason for the different rates of stratospheric cooling in the two runs is more complex. As shown in Figures 1 and 9, in run TRANS, tropical upwelling increases and stratospheric ozone decreases with time. All three factors, ozone depletion, increased upwelling, and greenhouse gas increase work in the same direction to cool the stratosphere on the timescale of the experiment. In contrast, run FUTUR exhibits a smaller rate of increase in upwelling (some cooling), a trend in ozone that is mostly zero or positive (warming), and a stronger increase in greenhouse gases (cooling). Consequently, the sum of the three factors leads to less stratospheric cooling than in TRANS.

[48] These results, based on the conceptual model, are qualitatively in good agreement with the regression analysis. This showed that in the past (TRANS), the dominating factors are stratospheric ozone depletion for tropopause temperature change and increased upwelling for tropopause height change, both of which are associated with stratospheric cooling.

[49] For the future (FUTUR), regression analysis indicates that SST and ozone change dominate the temperature response of the tropopause, with upwelling playing a secondary role. Again, this agrees well with our findings from the conceptual model that strong tropospheric warming and modest stratospheric cooling are responsible for the change in tropopause temperatures.

[50] Regarding the future tropopause height change, the conceptual model again suggests that tropospheric warming is the main driver whereas the regression analysis points to increased upwelling as the major factor. As noted before, this discrepancy can be explained by the fact that increased upwelling and tropospheric warming are ultimately caused

by the same climate change mechanisms, albeit with ozone change contributing additionally to the upwelling.

8. Discussion

[51] In this work we have used regression and a conceptual model of the tropopause to analyze the model results. While regression can only give an indication of the processes leading to tropopause change, the conceptual model has been complementary in establishing the physical processes which have led to the modeled changes. In principle an alternative procedure to identify the causes of tropopause change would have been to design a set of experiments with certain processes excluded. However, for the length and complexity of integrations used here, this would have proved impractical. In any case, in the coupled system that we are working with this would not necessarily have provided any clearer understanding of the processes involved. Further aspects of the model results are discussed here.

8.1. A Possible Relationship Between Tropopause Height and Age of Air

[52] The regression analysis suggests that both tropopause height and pressure are primarily driven by the tropical mass upwelling in the lower stratosphere. This provides a useful connection to previous studies on the tropical upwelling. For example *Butchart and Scaife* [2001] and *Butchart et al.* [2006] show that an increase in tropical mass upwelling occurs in most of those models examined which simulate climate change. It may therefore be expected that the increase in the height of the tropopause would be a qualitatively robust feature of climate change in general. Indeed this is confirmed by the results of Son et al. (submitted manuscript, 2008). Furthermore, similar qualitative relationships between the model results appear to apply. For example, AMTRAC has a larger change in age of air than the Whole Atmosphere Community climate Model (WACCM) [*Garcia et al.*, 2007]. Since age of air is inversely related to tropical upwelling [*Austin and Li*, 2006], WACCM would be expected to show smaller trends in tropical tropopause pressure than AMTRAC, as indeed is confirmed by Son et al. (submitted manuscript, 2008). These results suggest that the tropopause height could equally well be considered related to the age of air in the regression analysis. These arguments would suggest strong dynamical connections controlling the tropical tropopause pressure in our model. However, as shown by *Li et al.* [2008] ozone change can produce an indirect effect on tropical upwelling (and by implication age of air).

8.2. Relationship Between Tropopause Temperature and Water Vapor

[53] As noted in section 1, the tropopause temperature has a significant influence on stratospheric water vapor. Figure 11 shows the model water vapor near the hygropause and is compared with the saturated vapor mixing ratio at the tropopause. Before the year 2000, when volcanic eruptions were significantly influencing the model results, the model water vapor changed only by about 10%. After 2000 when the volcanic aerosol amount was specified at background level, the model hygropause mixing ratio is seen to be very closely related to the saturated mixing ratio at the tropopause
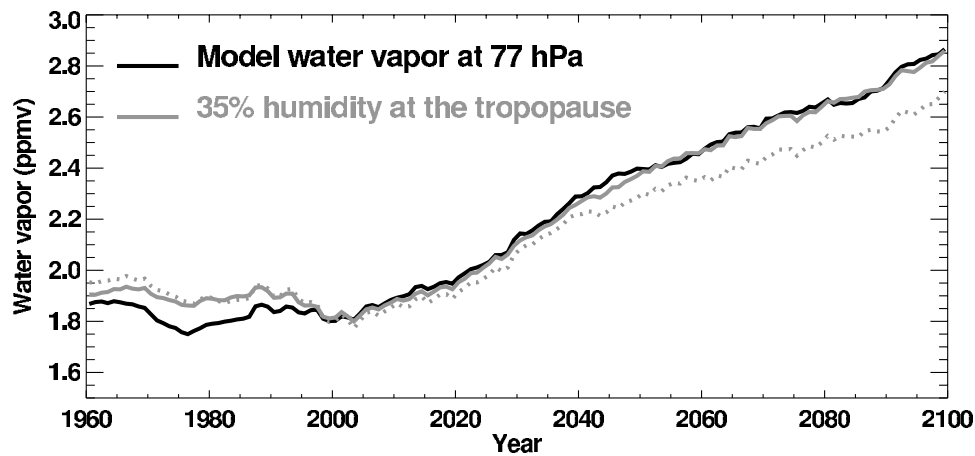
Figure 11. Model water vapor at the equator at 77 hPa (black), compared with 35% of the saturated mixing ratio at the tropopause (gray) for the model simulations. The model results are the ensemble mean values, shown as an 11 year running mean. The saturated mixing ratio values were calculated monthly and then averaged in time. The dotted line shows the 35% humidity line but without taking into account the change in pressure of the tropopause.

until the end of the century. The results obtained for a tropopause pressure equal to the year 2000 are shown by the dotted line in Figure 11, which steadily diverges from the model water vapor concentration.

[54] As expected, the negative trend in cold point pressure leads to increased saturation mixing ratio at the tropopause and thus in the stratosphere above. This clearly demonstrates that besides the temperature, the pressure at the cold point also controls to a smaller extent the amount of water vapor entering the stratosphere. It is also interesting to note that in the current case (Figure 11), both increasing temperatures and decreasing pressure work together to increase stratospheric water vapor amounts.

8.3. Relationship Between Tropopause Temperature and SSTs

[55] The regression analysis of tropical tropopause temperature contrasts with pressure and height in emphasizing more the direct effect of ozone change. An additional important term is due to the SST changes, and the tropical upwelling provides a smaller term. Both the upwelling and the SST terms are here found to be correlated with tropical tropopause temperature over multidecadal timescales. This is likely to be due to the expectation that climate change increases SSTs and the strength of the Brewer-Dobson circulation [*Butchart and Scaife*, 2001]. With the long-term trends removed, the opposite is seen in the model results, see for example Figure 12 which shows a clear anticorrelation between tropopause temperature and surface temperature on interannual timescales. This is also confirmed by Figure 5 which shows a change from an anticorrelation between SSTs and tropical tropopause temperature over timescales less than about 45 years and a correlation at timescales greater than about 50 years. The short term behavior indicates the expected physical effect
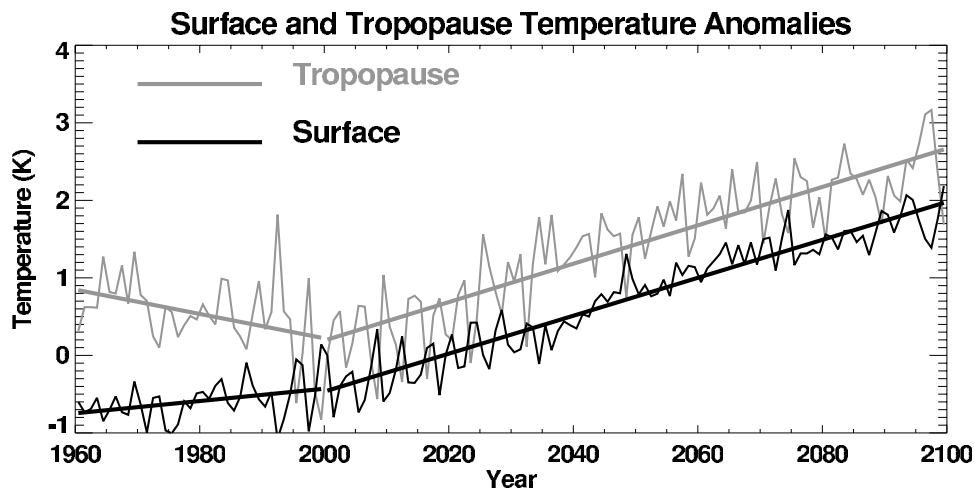
Figure 12. Comparison between the surface temperature (black) and tropopause temperatures (gray) for the first ensemble member. The values plotted are anomalies relative to the year 2000 mean and are annually averaged. The thinner lines are the year to year changes and the thicker lines are linear trend lines through the data, separated into the two periods pre and post 2000.

of an increase in SSTs leading to increased upward motion and upper tropospheric cooling and is consistent with the analysis of *Rosenlof and Reid* [2008] based on observations. Similarly, in the short term, upwelling and tropopause temperature are anticorrelated [*Randel et al.*, 2006], but over climate timescales the terms become correlated (Figure 5).

9. Conclusion

[56] Coupled chemistry climate model simulations for the period 1960 to 2100 have shown significant changes in the tropical tropopause height, pressure, and temperature. The model is in broad agreement with observations, although the latter are subject to large sampling errors. The tropopause pressure and height were found to follow the variations in the tropical mass upwelling. Overall, the tropopause height increased at 63 ± 3 m/decade and the tropopause pressure decreased at mean rates of 1.0 ± 0.3 hPa/decade in the past and 0.55 ± 0.06 hPa/decade in the future. Although in both cases the changes are dominated by tropical upwelling, atmospheric chemistry has played a role indirectly in the results through the ozone influence of the tropical upwelling. A relation was established between tropopause height and tropopause pressure changes. Analysis of the results showed that the past increase in the tropopause height in the model arose primarily from local, near tropopause changes. For the future simulations, tropospheric expansion due to global warming, and local changes were approximately equally important and height and pressure changes were shown to be linearly related to first order.

[57] The model tropopause temperature decreased for the period 1960–1999 at -0.13 ± 0.07 K/decade and increased for the period 2000–2099 at 0.254 ± 0.014. The results were analyzed using linear regression, which suggested that ozone depletion was important in the past, in agreement with the results of *Santer et al.* [2003]. The marked change in tropopause trends near the year 2000 was found to be related to the change in importance in the ozone and SSTs in driving the tropopause temperature. Another study which looked at tropopause height instead [*Sausen and Santer*, 2003] concluded that the tropopause height is an indicator of tropospheric climate change. Our results would tend to contradict this, since we show that tropopause height is related to tropical upwelling which itself has a significant ozone contribution [*Li et al.*, 2008]. Hence, ozone recovery without climate change would also lead to tropopause height increases.

[58] Results have also been presented from a detailed analysis of our results using the framework of the *Shepherd* [2002] conceptual model of the tropopause. To calculate trends, the conceptual model needs the temperature lapse rate in the troposphere and stratosphere to be specified. The conceptual model is consistent with the analysis obtained from examining the model tropopause trends directly. In particular, height and temperature trends using the conceptual model agree best with the actual model trends when those trends are taken from the upper troposphere and lower stratosphere. The agreement is then typically 10 m/decade for the tropopause height trend and 0.05 K/decade for the tropopause temperature

trend; compare the "ACTUAL" results with the UT/LS results in Figure 10.

[59] In the future, the recovery of ozone contributes to an increase in the tropopause temperature mostly due to radiative processes and in the regression analysis ozone change is the dominating factor until about 2040. Thereafter the SST impact exceeds the ozone impact and plays an increasing role. On these climate timescales increases in GHG concentrations have led to tropospheric temperature increases which are reflected in the SSTs. Overall, both linear regression methods and the conceptual model of the tropopause described by *Shepherd* [2002] have proved effective in helping to understand the behavior of the tropical cold point tropopause, especially its temperature. The two approaches were found to be complementary, with the regression analysis indicating how variations of the tropopause may have arisen, and with the conceptual model interpreting the changes in more physically direct ways, in terms of the temperature trends above and below the tropopause. Nonetheless, understanding has been hampered by an apparent "separation of timescales," whereby the tropopause temperature is anticorrelated with certain drivers (upwelling, SSTs) over timescales less than about 50 years or more but correlated over long timescales. This makes removal of the long-term trends from the fields less effective in understanding the origin of tropopause trends. Finally, the importance of the cold point tropopause has been confirmed in the simulations by showing that in the absence of volcanic eruptions, the humidity at the hygropause was closely related to the water vapor saturated mixing ratio at the tropopause.

References

Alexander, M. J., and T. J. Dunkerton (1999), A spectral parameterization of mean flow forcing due to breaking gravity waves, *J. Atmos. Sci.*, *56*, 4167–4182.

Anderson, J. L., et al. (2004), The new GFDL global atmosphere and land model AM2/LM2: Evaluation with prescribed SST simulations, *J. Clim.*, *17*, 4641–4673.

Atticks, M. G., and G. D. Robinson (1983), Some features of the structure of the tropical tropopause, *Q. J. R. Meteorol. Soc.*, *109*, 295–308.

Austin, J., and N. Butchart (2003), Coupled chemistry-climate model simulations for the period 1980 to 2020: ozone depletion and the start of ozone recovery, *Q. J. R. Meteorol. Soc.*, *129*, 3225–3249.

Austin, J., and F. Li (2006), On the relationship between the strength of the Brewer-Dobson circulation and the age of stratospheric air, *Geophys. Res. Lett.*, *33*, L17807, doi:10.1029/2006GL026867.

Austin, J., and R. J. Wilson (2006), Ensemble simulations of the decline and recovery of stratospheric ozone, *J. Geophys. Res.*, *111*, D16314, doi:10.1029/2005JD006907.

Birner, T. (2006), Fine-scale structure of the extratropical tropopause region, *J. Geophys. Res.*, *111*, D04104, doi:10.1029/2005JD006301.

Butchart, N., and A. A. Scaife (2001), Removal of chlorofluorocarbons by increased mass exchange between the stratosphere and the troposphere in a changing climate, *Nature*, *410*, 799–802.

Butchart, N., et al. (2006), Simulation of anthropogenic change in the strength of the Brewer-Dobson Circulation, *Clim. Dyn.*, *27*, 727–741.

Delworth, T. L., et al. (2006), GFDL's CM2 global coupled climate models - Part 1: Formulation and simulation characteristics, *J. Clim.*, *19*, 643–674.

Eyring, V., et al. (2006), Assessment of coupled chemistry-climate models: Evaluation of dynamics, transport and ozone, *J. Geophys. Res.*, *111*, D22308, doi:10.1029/2006JD007327.

Fomichev, V. I., A. I. Johnson, J. de Grandpré, S. R. Beagley, C. McLandress, K. Semeniuk, and T. G. Shepherd (2007), Response of the middle atmosphere to CO_2 doubling: Results from the Canadian middle atmosphere model, *J. Clim.*, *20*, 1121–1144.

Forster, P. M. D., and K. P. Sine (2002), Assessing the climate impact of trends in stratospheric water vapor, *Geophys. Res. Lett.*, *29*(6), 1086, doi:10.1029/2001GL013909.

Garcia, R. R., D. R. Marsh, D. E. Kinnison, B. A. Boville, and F. Sassi (2007), Simulation of secular trends in the middle atmosphere, *J. Geophys. Res.*, *112*, D09301, doi:10.1029/2006JD007485.

Gettelman, A., et al. (2008), The tropical tropopause layer 1960–2100, *Atmos. Chem. Phys. Discuss.*, *8*, 1367–1413.

Intergovernmental Panel on Climate Change (2001), *Climate Change 2001: The Scientific Basis*, edited by J. T. Houghton et al., 881 pp., Cambridge Univ. Press, New York.

Knutson, T. R., T. L. Delworth, K. W. Dixon, I. M. Held, J. Lu, V. Ramaswamy, M. D. Schwarzkopf, G. Stenchikov, and R. J. Stouffer (2006), Assessment of twentieth-century regional surface temperature trends using the GFDL CM2 coupled models, *J. Clim*, *19*, 1624–1651.

Li, F., J. Austin, and R. J. Wilson (2008), The strength of the Brewer-Dobson Circulation in a changing climate: A coupled chemistry-climate model simulation, *J. Clim.*, *21*, 40–57.

Numerical Algorithms Group (1999), NAG Fortran library, mark 19, Oxford, U. K.

Randel, W. J., F. Wu, and W. Rivera-Rios (2003), Thermal variability of the tropical tropopause region derived from GPS/MET observations, *J. Geophys. Res.*, *108*(D1), 4024, doi:10.1029/2002JD002595.

Randel, W. J., F. Wu, H. Vömel, G. E. Nedoluha, and P. Forster (2006), Decreases in stratospheric water vapor after 2001: Links to changes in the tropical tropopause and the Brewer-Dobson circulation, *J. Geophys. Res.*, *111*, D12312, doi:10.1029/2005JD006744.

Reichler, T., M. Dameris, and R. Sausen (2003), Determining the tropopause height from gridded data, *Geophys. Res. Lett.*, *30*(20), 2042, doi:10.1029/2003GL018240.

Rood, R. B. (2005), Assimilation of stratospheric meteorological and constituent observations: A review, *SPARC Newsl.*, *25*, 31–37.

Rosenlof, K., and G. C. Reid (2008), Trends in the temperature an water vapor content of the tropical lower stratosphere: The sea-surface connection, *J. Geophys. Res.*, *113*, D06107, doi:10.1029/2007JD009109.

Santer, B. D., et al. (2003), Contributions of anthropogenic and natural forcing to recent tropopause height changes, *Science*, *301*, 479–483.

Santer, B. D., et al. (2004), Identification of anthropogenic climate change using a second-generation reanalysis, *J. Geophys. Res.*, *109*, D21104, doi:10.1029/2004JD005075.

Sausen, R., and B. D. Santer (2003), Use of changes in tropopause height to detect human influences on climate, *Meteorol. Z.*, *12*, 131–136.

Schnadt, C., and M. Dameris (2003), Relationship between North Atlantic Oscillation changes and stratospheric ozone recovery in the northern hemisphere in a chemistry-climate model, *Geophys. Res. Lett.*, *30*(9), 1487, doi:10.1029/2003GL017006.

Seidel, D. J., and W. J. Randel (2006), Variability and trends in the global tropopause estimated from radiosonde data, *J. Geophys. Res.*, *111*, D21101, doi:10.1029/2006JD007363.

Seidel, D. J., R. J. Ross, J. K. Angell, and G. C. Reid (2001), Climatological characteristics of the tropical tropopause as revealed by radiosondes, *J. Geophys. Res.*, *106*, 7857–7878.

Shepherd, T. G. (2002), Issues in stratosphere-troposphere coupling, *J. Meteorol. Soc. Jpn.*, *80*, 769–792.

Staten, P. W., and T. Reichler (2008), An intercomparison of GPS-derived tropopause parameters, *J. Geophys. Res.*, *113*, D00B05, doi:10.1029/2008JD009886.

Thomason, L. W., and L. R. Poole (1997), A global climatology of stratospheric aerosol surface area density deduced from Stratospheric Aerosol and Gas Experiment II measurements: 1984–1994, *J. Geophys. Res.*, *102*, 8967–8976.

Thuburn, J., and G. C. Craig (2000), Stratospheric influence on tropopause height: The radiative constraint, *J. Atmos. Sci.*, *57*, 17–28.

Tiao, G. C., G. C. Reinsel, D. Xu, J. H. Pedrick, X. Zhu, A. J. Miller, J. J. DeLuisi, C. L. Mateer, and D. J. Wuebbles (1990), Effects of autocorrelation and temporal sampling schemes on estimates of trend and spatial correlation, *J. Geophys. Res.*, *95*, 20,507–20,517.

World Meteorological Organization (WMO) (1957), Meteorology, a three-dimensional science: Second session of the Commission for Aerology, *WMO Bull.*, *IV*(4), 134–138.

WMO (2003), Scientific assessment of ozone depletion: 2002, *Rep. 47*, Geneva.

Yulaeva, E., J. R. Holton, and J. M. Wallace (1994), On the cause of the annual cycle in tropical lower-stratospheric temperatures, *J. Atmos. Sci.*, *51*, 169–174.

_____

J. Austin, Geophysical Fluid Dynamics Laboratory, 201 Forrestal Road, Princeton, NJ 08542-0308, USA. (john.austin@noaa.gov)

T. J. Reichler, Department of Meteorology, University of Utah, William Browning Building, Room 819, Salt Lake City, UT 84112-0110, USA.